Suplemento de la Revista Mexicana de Física **4** 021121 (2023) 1–4

Exclusive photo-production of J/Ψ and $\Psi(2s)$ as a tool to explore the transition to high and saturated gluon densities at the LHC

M. Alcazar Peredo and M. Hentschinski

Departamento de Actuaria, Física y Matemáticas, Universidad de las Américas Puebla, Ex-Hacienda Santa Catarina Martir S/N, San Andrés Cholula, 72820 Puebla, México.

Received 30 May 2023; accepted 11 August 2023

We study the energy dependence of the cross-section for exclusive photo-production of vector mesons J/Ψ and $\Psi(2s)$ and search for signs for the onset of non-linear QCD dynamics in this observable. Our study is based on two dipole models: the Golec-Biernat, Wuesthoff Model (GBW) and the Bartels, Golec-Biernat, Kowalski Model (BGK). We find that differences between linear and non-linear implementations of these models are relatively small in the kinematic region probed by both HERA and LHC experiments if the energy dependence of the photoproduction cross-section is being considered. We however find that the ratio of both cross-sections grows with energy in the presence of non-linear effects, while it remains approximately constant in the linearized case. The ratio of photo-production cross-sections might therefore provide a suitable tool to characterize the size of non-linear QCD effects at current collider energies.

Keywords: Quantum chromodynamics; deep inelastic scattering; large hadron collider; forward physics; ultra-peripheral collisions; gluon distribution.

DOI: https://doi.org/10.31349/SuplRevMexFis.4.021121

1. Introduction

To attempt a description of a hadronic reaction based on perturbative Quantum Chromodynamics (QCD) the presence of a so-called hard scale Q which is significantly larger than the QCD characteristic scale $\Lambda_{\rm QCD}$ of the order of a few hundred MeV is indispensable. The presence of such a hard scale renders the strong coupling constant α_s small, allowing furthermore to identify partonic degrees of freedom (quarks, gluons) in the hadron. This procedure however works only well as long as the density of quarks and gluons is not large. The latter scenario is potentially realized in the so-called low x limit, where $x \approx Q^2/W^2 \ll 1$. The primary goal of this work is to study the energy dependence of the exclusive photoproduction of vector mesons and to identify observables that can distinguish between gluon distributions subject to linear and non-linear QCD evolution.

Dipole models are a powerful tool to provide a first description of both inclusive and diffractive deep inelastic scattering cross sections in HERA and LHC detectors in this limit, due to the fact that they provide an excellent description of QCD reactions at low-x and in the low Q^2 region. [1, 2].

In photon-induced reactions at low x, such as Deep Inelastic Scattering of electrons and protons or ultra-peripheral collisions of two hadrons, such dipole models assume the splitting of the initial photon into a quark-antiquark pair. Dipole models then describe the eikonal interaction of this color dipole with the high-density gluonic field of the target hadron. To determine the probability of finding a dipole of transverse size r within a photon and the subsequent transition to a vector meson, one additionally requires the corresponding light-front wave function overlap, which describes the formation of the dipole and its annihilation into a certain final state. The scattering amplitude is then defined as the convolution of the wave function overlap and the dipole cross-section $\sigma_{q\bar{q}}$.

2. Formalism

With W the center of mass energy of the photon-proton collision and t the momentum transfer we have for the differential cross-section [3]:

$$\frac{d\sigma}{dt}(\gamma p \to Vp) = \frac{1}{16\pi} \mid A^{\gamma p \to Vp}(W^2, t) \mid, \qquad (1)$$

where $A(W^2, t)$ denotes the scattering amplitude for the reaction $\gamma p \to Vp$ with $V = J/\Psi, \Psi(2s)$ the vector meson. At high center of mass energies, the dominant contribution to the scattering amplitude is given by its imaginary part. Corrections due to the real part of the scattering amplitude can be estimated using dispersion relations as follows [4]:

$$\frac{\Re e A(W^2, t)}{\Im m A(W^2, t)} = \tan\left(\frac{\lambda\pi}{2}\right), \qquad (2)$$

with,

$$\lambda(x) = \frac{d}{d\ln(1/x)} \ln \Im m A(x, t).$$

In this work we do not assume a constant λ, but determine instead the slope λ from the x-dependent imaginary part of the scattering amplitude, see also [4–10].

2.1. Wave function overlap

The imaginary part of the scattering amplitude is obtained using:

$$\Im m A_T(W^2, t = 0) = \int d^2\mathbf{r}\, \sigma_{q\bar{q}}\left(\frac{M_V^2}{W^2}, r\right) \overline{\Sigma}_T(r), \qquad (3)$$

with $r = |\,\mathbf{r}\,|$. Here

$$\overline{\Sigma}_T(r) = \int_0^1 \frac{dz}{4\pi} \left(\psi_V^* \psi^*\right)_T (z, r), \tag{4}$$

where the wave function overlap of photon and vector meson wave function is given by

$$(\Psi_V^* \Psi)_T = \hat{e}_f e \frac{N_c}{\pi z(1-z)} \{m_f^2 K_0(\epsilon r)\phi_T(r,z) - [z^2 + (1-z)^2]\epsilon K_1(\epsilon r)\partial_r \phi_T(r,z)\}. \tag{5}$$

In the above expression, ϕ_T denotes the scalar wave function for which we use a simple Gaussian model, see [3] for the explicit form as well as [11] for the employed parameter set; T denotes the transverse polarization of the real photon.

Furthermore, $\hat{e}_f = 2/3$ for the charm quark and $e = \sqrt{4\pi\alpha_{e.m.}}$, whereas $\alpha_{e.m}$ is the electromagnetic fine structure constant, $N_c = 3$ is the number of colors and $K_{0,1}(\epsilon r)$. are the Bessel functions of the second kind, respectively.

2.2. Dipole models

The simplest saturation model is the GBW model [1] with a dipole cross-section:

$$\sigma_{q\bar{q}}(x, r) = \sigma_0 \left(1 - \exp\left[-\frac{r^2 Q_s^2(x)}{4}\right]\right). \tag{6}$$

Here, r corresponds to the transverse separation between the quark and the antiquark, and the saturation scale Q_s is parametrized as follows:

$$Q_s^2(x) = Q_0^2 \left(\frac{x_0}{x}\right)^{\lambda}. \tag{7}$$

In the following, we propose a modification to the non-linear version of this model and implement a parameter k which simulates non-linear effects through exponentiation of the leading order QCD description. The modified GBW Model reads:

$$\sigma_{q\bar{q}}(x, r, k) = \frac{\sigma_0}{k} \left(1 - \exp\left[\frac{-k \cdot r^2 Q_s^2(x)}{4}\right]\right), \tag{8}$$

where $k = 0$ yields the linearized model

$$\sigma_{q\bar{q}} = \sigma_0 r^2 Q_s^2 / 4.$$

The case $k = 1$ corresponds on the other hand to the complete non-linear fit of this model. Note that the parameter k has been inserted in a way such that it leaves the linearized model unmodified. It, therefore, serves as a tool to test the relevance of the non-linear terms. Including the same modification to the BGK model we have:

$$\sigma_{q\bar{q}}(x, r, k) = \frac{\sigma_0}{k} \cdot \left(1 - \exp\left[\frac{-k \cdot \pi^2 r^2 \alpha_s(\mu_r^2) x g(x, \mu_r^2)}{3\sigma_0}\right]\right). \tag{9}$$

Here, $xg(x, \mu^2)$ denotes the collinear gluon density which is parametrized at the starting scale μ_0^2 and evolves to scales μ^2 using leading order Dokshitzer-Gribov-Lipatov-Altarelli-Parisi (DGLAP) evolution, while $\alpha_s(\mu^2)$ denotes the QCD running coupling and σ_0 is a parameter of the model which gives the transverse size of the proton in the collision. For the description to work for large dipole sizes, one uses a dipole size dependent factorization scale as $\mu_r^2 = \mu_0^2/(1 - \exp\left(-\mu_0^2 r^2/C\right))$, while the gluon distribution is evolved with DGLAP evolution equations truncated to the gluonic sector,

$$\frac{\partial g(x, \mu^2)}{\partial \ln \mu^2} = \frac{\alpha_s(\mu^2)}{2\pi} \int_x^1 \frac{dz}{z} P_{gg}(x) g\left(\frac{x}{z}, \mu^2\right), \tag{10}$$

with an initial condition,

$$xg(x, Q_0^2) = A_g x^{-\lambda_g} (1-x)^{5.6}, \tag{11}$$

with $Q_0 = 1$ GeV and the gluon-to-gluon splitting function $P_{gg}(z)$, see [1] for details and values of parameters.

3. Comparison to data and conclusion

In Fig. 1 and 2, we compare our numerical results to HERA and LHC data. In particular, we explore for both models the effects of varying the parameter k away from the original $k = 1$, which corresponds to the underlying fit. For both models, if the parameter k is large, a stronger emphasis is given to non-linear terms, while the model turns essentially linear if $k \to 0$. Our result illustrates excellently the sensitivity of the observable to the presence/absence of non-linear effects. Introducing this simple parameter allows us therefore to evaluate further the relevance of non-linear corrections in the LHC region, in particular, if one assumes that those terms are only weakly constrained by HERA data.

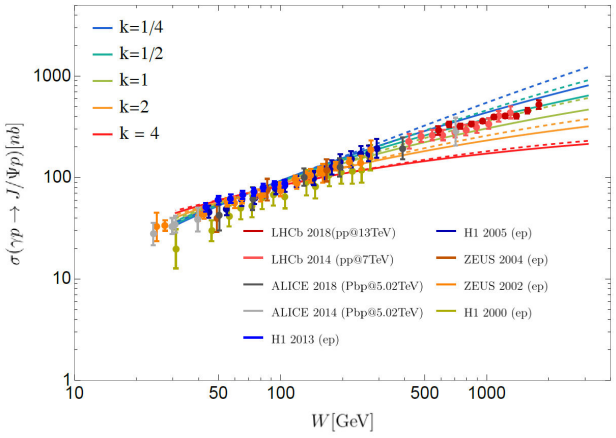

FIGURE 1. Top: The energy dependence of the J/Ψ photo-production cross-section provided by the BGK (solid) and GBW (dashed) saturation models. We further display photo-production data measured at HERA (ZEUS [12, 13], H1 [14–16]) as well as LHC data (ALICE [17, 18], LHCb [19, 20]).

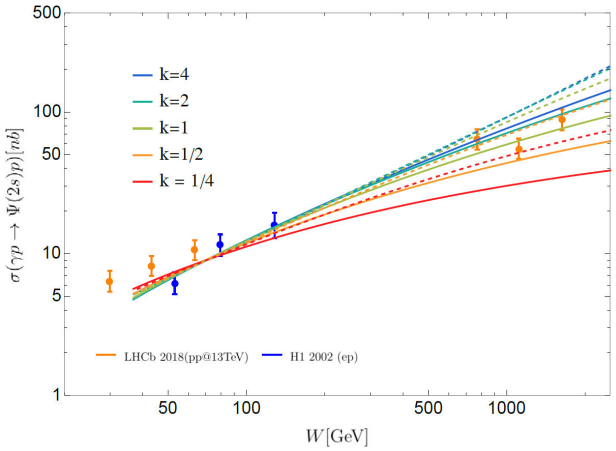

FIGURE 2. The same as Fig. 1, but for the $\Psi(2s)$ photo-production cross-section, with data measured by the H1 [14,21] and LHCb [21] collaborations.

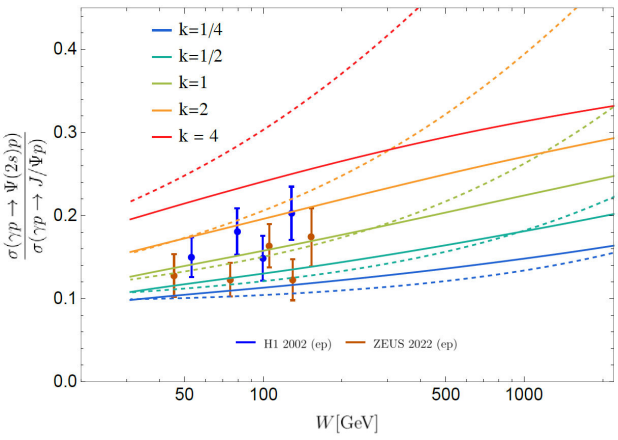

FIGURE 3. The energy dependence of the ratio of $\Psi(2s)$ and J/Ψ photo-production cross-section process provided by BGK (solid) and GBW (dashed) saturation models. We further display photo-production data measured at HERA (H1 [14], ZEUS [22]).

In Fig. 3 we finally consider the energy dependence of the ratio of $\Psi(2s)$ and J/Ψ photo-production cross-section process. In particular, we recover the observation made in Ref. [4] that the ratio of $\Psi(2s)$ and J/Ψ cross-section is approximately constant with energy W if non-linear effects are absent.

The complete study is currently in progress and will be reported separately.

1. K. Golec-Biernat and S. Sapeta, Saturation model of DIS: an update, *JHEP* **2018** (2018) 102, https://doi.org/10.1007/JHEP03(2018)102.
2. A. Luszczak and H. Kowalski, Dipole model analysis of highest precision HERA data, including very low Q^2, *Phys. Rev. D* **95** (2017) 014030, https://doi.org/10.1103/PhysRevD.95.014030.
3. H. Kowalski, L. Motyka, and G. Watt, Exclusive diffractive processes at HERA within the dipole picture, *Phys. Rev. D* **74** (2006) 074016. https://doi.org/10.1103/PhysRevD.74.074016.
4. M. Hentschinski and E. Padrón Molina, Exclusive J/ψ and ψ(2s) photo-production as a probe of QCD low x evolution equations, *Phys. Rev. D* **103** (2021) 074008, https://doi.org/10.1103/PhysRevD.103.074008.
5. I. Bautista, A. Fernandez Tellez, and M. Hentschinski, BFKL evolution and the growth with energy of exclusive J/ψ and Υ photoproduction cross sections, *Phys. Rev. D* **94** (2016) 054002, https://doi.org/10.1103/PhysRevD.94.054002.
6. A. Arroyo Garcia, M. Hentschinski, and K. Kutak, QCD evolution based evidence for the onset of gluon saturation in exclusive photo-production of vector mesons, *Phys. Lett. B* **795** (2019) 569, https://doi.org/10.1016/j.physletb.2019.06.061.
7. M. Hentschinski, QCD evolution based evidence for the onset of gluon saturation in exclusive photo-production of vector mesons, *PoS EPS-HEP* **2019** (2020) 528, https://doi.org/10.22323/1.364.0528.
8. M. Hentschinski and K. Kutak, Signs for the onset of gluon saturation in exclusive photo-production of vector mesons, *PoS LHCP* **2019** (2019) 039, https://doi.org/10.22323/1.350.0039.
9. M. Hentschinski, The use of QCD evolution to detect gluon saturation in exclusive photo-production of vector mesons, In Workshop of QCD and Forward Physics at the the LHC, the future Electron Ion Collider and Cosmic Ray Physics (University of Kansas Libraries, Lawrence, 2020) pp. 187-192.
10. M. A. Alcanzar Peredo, Exclusive Photon-production of J/Ψ and $\Psi(2s)$ as a tool to explore the transition to high and satured gluon densities at the LHC, (Tesis de licenciatura, Universidad de las Americas Puebla, 2022).
11. N. Armesto and A. H. Rezaeian, Exclusive vector meson production at high energies and gluon saturation, *Phys. Rev. D* **90** (2014) 054003, https://doi.org/10.1103/PhysRevD.90.054003.
12. S. Chekanov *et al.*, Exclusive photoproduction of J/ψ mesons at HERA, *Eur. Phys. J. C* **24** (2002) 345, https://doi.org/10.1007/s10052-002-0953-7.
13. S. Chekanov *et al.*, Exclusive electroproduction of J/ψ mesons at HERA, *Nucl. Phys. B* **695** (2004) 3, https://doi.org/10.1016/j.nuclphysb.2004.06.034.
14. C. Adloff *et al.*, Diffractive photoproduction of $\psi(2S)$ mesons at HERA, *Phys. Lett. B* **541** (2002) 251, https://doi.org/10.1016/S0370-2693(02)02275-X.
15. T. H. Collaboration, *et al.*, Elastic J/ψ production at HERA, *Eur. Phys. J. C* **46** (2006) 585, https://doi.org/10.1140/epjc/s2006-02519-5.

16. C. Alexa *et al.*, Elastic and Proton-Dissociative Photoproduction of J/ψ Mesons at HERA, *Eur. Phys. J. C* **73** (2013) 2466, https://doi.org/10.1140/epjc/s10052-013-2466-y.

17. B. Abelev *et al.*, Exclusive J/ψ photoproduction off protons in ultra-peripheral p-Pb collisions at $\sqrt{sNN} = 5.02$ TeV, *Phys. Rev. Lett.* **113** (2014) 232504, https://doi.org/10.1103/PhysRevLett.113.232504.

18. S. Acharya *et al.*, Energy dependence of exclusive J/ψ photoproduction off protons in ultra-peripheral p-Pb collisions at $\sqrt{sNN} = 5.02$ TeV, *Eur. Phys. J. C* **79** (2019) 402, https://doi.org/10.1140/epjc/s10052-019-6816-2.

19. R. Aaij *et al.*, Exclusive J/ψ and $\psi(2S)$ production in pp collisions at $\sqrt{s} = 7$ TeV, *J. Phys. G: Nucl. Part. Phys.* **40** (2013) 045001, https://doi.org/10.1088/0954-3899/40/4/045001.

20. R. Aaij *et al.*, Central exclusive production of J/ψ and ψ(2S) mesons in pp collisions at $\sqrt{s} = 13$ TeV, *JHEP* **5018** (2018) 167, https://doi.org/10.1007/JHEP10(2018)167.

21. D. Schmidt, Diffractive photoproduction of charmonium in the H1 detector at HERA, Ph. D. thesis, Hamburg U. (2001).

22. Zeus Collaboration, Measurement of the cross-section ratio $\sigma_{\Psi(2S)}/\sigma_{J/\Psi(1S)}$ in exclusive photoproduction at HERA (2022), https://doi.org/10.48550/ARXIV.2206.13343.